MMSE ADAPTIVE WAVEFORM DESIGN FOR A MIMO ACTIVE SENSING SYSTEM TRACKING MULTIPLE MOVING TARGETS

Steven Herbert, James Hopgood, Bernard Mulgrew

Institute for Digital Communications, School of Engineering, University of Edinburgh, Edinburgh, UK.

ABSTRACT

This paper proposes a method for minimum mean squared error (MMSE) adaptive waveform design (AWD) in multiple-input-multiple-output (MIMO) active sensing systems which are used to track moving targets. The method proposed herein prompts two computational improvements compared to a related method for static targets. Consideration of moving targets also introduces the possibility of 'model mismatch' between the actual motion of the targets, and the model available to the MMSE AWD system. Results show that the proposed method leads to an improvement in mean squared error performance of up to 29% compared to the non-adaptive case.

Index Terms— Adaptive waveform design, optimal design, MMSE, MIMO, active sensing

1. INTRODUCTION

Active sensing systems have the definitive property that energy is transmitted and reflected off one or more targets which is received and used to gain information about parameters associated with these targets. This motivates the key question of how best to transmit energy to maximise the information gain. Prior research on this has primarily concerned radar as the active sensing modality, known as *cognitive radar*, and various articles provide a good overview of this topic [1–3].

More specifically, Huleihel *et al* include a schematic diagram of an active sensing architecture that is generally applicable [4, Fig. 1]. This active sensing formulation is a good fit for spatial waveform shaping using multiple-input-multiple-output (MIMO) active sensing systems, for example, MIMO radar and sonar [5], which is our focus in this paper. A number of criteria have been proposed to define what is meant by *maximising the information gain* concerning the target parameters, including maximising the mutual information [6–8], maximising the signal-to-noise ratio [9–12] and minimising the mean squared error of the target parameter estimation (MMSE estimation) [13]. These criteria can be interpreted in terms of optimal experimental design [14], leading to the conclusion that MMSE (A-optimal) estimation is a good criterion in general [15].

So it follows that we consider MMSE adaptive waveform design (AWD) in this paper. [13] expresses analytically the cost function for MMSE AWD, and demonstrates how MMSE AWD can be practically implemented using numerical sums to approximate the integrals present in the aforementioned cost function. Notably, [13] considers only static targets (as the purpose was to use a simple set-up to prove the principle of the method proposed therein), and in this paper we build on the analysis in [13] to enable MMSE AWD for moving targets and thus make an important step towards developing a physically representative MMSE AWD method. Additionally, this shift from a static to a dynamic setting prompts some theoretical refinements in the MMSE AWD method and the particle filter (PF), which conducts the underlying Bayesian estimation of the target parameters, leading to a reduction in the computational complexity. Finally, the formulation we present incorporates the possibility of a discrepancy between the actual motion of the targets and the model of target motion available to the MIMO sensing system, and results show that our MMSE AWD method is effective both with and without such a model mismatch.

2. SYSTEM MODEL

We start with the standard MIMO active sensing system formulation [16] (with N_T transmission elements, N_R receiving elements and L snapshots per step):

$$\mathbf{X}_k = \mathbf{H}_k(\boldsymbol{\theta}_k)\mathbf{S}_k + \mathbf{N}_k, \tag{1}$$

where $\mathbf{S}_k \in \mathbb{C}^{N_T \times L}$ is the transmitted waveform, $\mathbf{X}_k \in \mathbb{C}^{N_R \times L}$ is the received waveform, $\mathbf{N}_k \in \mathbb{C}^{N_R \times L}$ is additive white Gaussian noise, $\mathbf{H}_k \in \mathbb{C}^{N_R \times N_T}$ represents the channel response as a non-linear function (in general) of $\boldsymbol{\theta}_k = [\Re(\boldsymbol{\alpha}_k); \Im(\boldsymbol{\alpha}_k); \boldsymbol{\phi}_k]$ in which $\boldsymbol{\alpha}_k$ and $\boldsymbol{\phi}_k$ are vectors of complex attenuations and angles of the Q' targets respectively, i.e., $\boldsymbol{\alpha}_k \in \mathbb{C}^{Q' \times 1}$, $\boldsymbol{\phi}_k \in \mathbb{R}^{Q' \times 1}$. This enables us to define:

$$\mathbf{H}_k = \sum_{q=1}^{Q'} [\boldsymbol{\alpha}_k]_q \mathbf{a}_R([\boldsymbol{\phi}_k]_q)\mathbf{a}_T^T([\boldsymbol{\phi}_k]_q), \tag{2}$$

where $\mathbf{a}_R \in \mathbb{C}^{N_R \times 1}$ and $\mathbf{a}_T \in \mathbb{C}^{N_T \times 1}$ are the steering vectors for the receive and transmit arrays respectively.

This work was supported by the Engineering and Physical Sciences Research Council (EPSRC) Grant number EP/K014277/1 and the MOD University Defence Research Collaboration (UDRC) in Signal Processing.

3. MMSE AWD METHOD FOR STATIC TARGETS

First we summarise the MMSE AWD method for static targets [13], which we will subsequently generalise to apply to the moving target scenario. Starting with the expected covariance matrix, first expressed in [13, Eq. (11)] [1]:

$$\Sigma_k = \iint (\hat{\boldsymbol{\theta}}_k - \boldsymbol{\theta}_k)(\hat{\boldsymbol{\theta}}_k - \boldsymbol{\theta}_k)^T \\ p(\boldsymbol{\theta}_k|\mathbf{X}^{k-1}, \mathbf{S}^{k-1})p(\mathbf{X}_k|\boldsymbol{\theta}_k, \mathbf{S}_k)\,\mathrm{d}\mathbf{X}_k\,\mathrm{d}\boldsymbol{\theta}_k, \quad (3)$$

where $\hat{\boldsymbol{\theta}}_k = \mathbb{E}(\boldsymbol{\theta}_k|\mathbf{X}_k, \mathbf{X}^{k-1}, \mathbf{S}_k, \mathbf{S}^{k-1})$, i.e., the expected estimate of $\boldsymbol{\theta_k}$, itself a random variable. Which in turn enables the MMSE optimisation cost function to be expressed:

$$\begin{array}{lll} \text{minimise:} & \mathrm{tr}(\Sigma_k) & \text{w.r.t. } \mathbf{S}_k \\ \text{subject to:} & \mathrm{tr}\left(\frac{1}{L}\mathbf{S}_k\mathbf{S}_k^H\right) \leq \mathrm{P} & \end{array} \quad (4)$$

where $\mathrm{tr}(.)$ is the matrix trace operation and P is the total transmit power per step. A particle filter (PF) was used to estimate the probability density function (PDF) of the target parameters at each step ([13] initialised the PF particles on a regular grid and didn't resample):

$$p(\boldsymbol{\theta}_k) \approx \sum_{i=1}^{N_P} w_k^{(i)} \delta(\boldsymbol{\theta}_k - \boldsymbol{\theta}_k^{(i)}), \quad (5)$$

where w_k is the weight of the kth particle, $\boldsymbol{\theta}_k^{(i)}$. The PF was itself sampled, to give an additional random set of size N_S (by definition); for the mth sample:

$$\begin{array}{lcl} \boldsymbol{\theta}_k'^{(m)} & \sim & \sum_{i=1}^{N_P} w_k^{(i)} \delta(\boldsymbol{\theta}_k'^{(m)} - \boldsymbol{\theta}_k^{(i)}) \\ \mathbf{X}_k^{(m)} & \sim & p(\mathbf{X}_k^{(m)}|\boldsymbol{\theta}_k'^{(m)}, \mathbf{S}_k(0)) \end{array}. \quad (6)$$

These definitions were used to numerically approximate the cost function. To do so, it was convenient to use vectorised forms of $\mathbf{S}_k$ and $\mathbf{X}_k$ split into real and imaginary components: $\mathbf{s}_k' \triangleq [\Re(\mathrm{vec}(\mathbf{S}_k)); \Im(\mathrm{vec}(\mathbf{S}_k))]$ and similarly for $\mathbf{X}_k$. $\mathbf{H}_k''$ was defined as L copies of $\mathbf{H}_k$ positioned on the leading diagonal of a larger matrix, whose other elements are all zero, from which $\mathbf{H}_k' \triangleq [\Re(\mathbf{H}_k''), -\Im(\mathbf{H}_k''); \Im(\mathbf{H}_k''), \Re(\mathbf{H}_k'')]$ was also defined. This led to the expression:

$$\Sigma_k \approx \Sigma_k'' = \sum_{m=1}^{N_S} \frac{v_m}{\tilde{v}} \mathbf{u}_m^T \mathbf{u}_m, \quad (7)$$

where:

$$v_m = \frac{p(\mathbf{x}_k'^{(m)}|\boldsymbol{\theta}_k'^{(m)}, \mathbf{s}_k')}{p(\mathbf{x}_k'^{(m)}|\boldsymbol{\theta}_k'^{(m)}, \mathbf{s}_k'(0))}, \quad (8)$$

$$\tilde{v} = \sum_{m'=1}^{N_S} \frac{p(\mathbf{x}_k'^{(m')}|\boldsymbol{\theta}_k'^{(m')}, \mathbf{s}_k')}{p(\mathbf{x}_k'^{(m')}|\boldsymbol{\theta}_k'^{(m')}, \mathbf{s}_k'(0))}, \quad (9)$$

$$\mathbf{u}_m = \left(\frac{\sum_{i=1}^{N_P} w_k^{(i)} p(\mathbf{x}_k'^{(m)}|\boldsymbol{\theta}_k^{(i)}, \mathbf{s}_k')\boldsymbol{\theta}_k^{(i)}}{\sum_{i=1}^{N_P} w_k^{(i)} p(\mathbf{x}_k'^{(m)}|\boldsymbol{\theta}_k^{(i)}, \mathbf{s}_k')} - \boldsymbol{\theta}_k'^{(m)} \right). \quad (10)$$

[1] this expression is the exact cost function of which Huleihel *et al* optimise a lower bound [4, Eq. (6)]

The MMSE AWD method used gradient descent to optimise the cost function, therefore it was also necessary to express:

$$\nabla_{\mathbf{s}_k'}(\Sigma_k'') = \sum_{m=1}^{N_S} \frac{v_m}{\tilde{v}} \nabla_{\mathbf{s}_k'}(\mathbf{u}_m^T\mathbf{u}_m) \\ + \frac{\tilde{v}\nabla_{\mathbf{s}_k'}(v_m) - v_m\nabla_{\mathbf{s}_k'}(\tilde{v})}{\tilde{v}^2}\mathbf{u}_m^T\mathbf{u}_m, \quad (11)$$

a single element of $\nabla_{\mathbf{s}_k'}(\mathbf{u}_m^T\mathbf{u}_m)$ is expressed in (12), also:

$$\nabla_{\mathbf{s}_k'}(v_m) = \frac{\nabla_{\mathbf{s}_k'}(p(\mathbf{x}_k'^{(m)}|\boldsymbol{\theta}_k'^{(m)}, \mathbf{s}_k'))}{p(\mathbf{x}_k'^{(m)}|\boldsymbol{\theta}_k'^{(m)}, \mathbf{s}_k'(0))} \quad (13)$$

$$\nabla_{\mathbf{s}_k'}(\tilde{v}) = \sum_{m'=1}^{N_S} \frac{\nabla_{\mathbf{s}_k'}(p(\mathbf{x}_k'^{(m')}|\boldsymbol{\theta}_k'^{(m')}, \mathbf{s}_k'))}{p(\mathbf{x}_k'^{(m')}|\boldsymbol{\theta}_k'^{(m')}, \mathbf{s}_k'(0))}, \quad (14)$$

where:

$$p(\mathbf{x}_k'|\boldsymbol{\theta}_k, \mathbf{s}_k') = \frac{\exp(-(\mathbf{x}_k' - \mathbf{H}_k'\mathbf{s}_k')^T\mathbf{R}_n^{-1}(\mathbf{x}_k' - \mathbf{H}_k'\mathbf{s}_k'))}{\sqrt{(2\pi)^{2N_R}\det(\mathbf{R}_n)}}, \quad (15)$$

and

$$\nabla_{\mathbf{s}_k'}(p(\mathbf{x}_k'|\boldsymbol{\theta}_k, \mathbf{s}_k')) \\ = 2p(\mathbf{x}_k'|\boldsymbol{\theta}_k, \mathbf{s}_k')\left(\mathbf{H}_k'^T\mathbf{R}_n^{-1}\mathbf{x}_k' - \mathbf{H}_k'^T\mathbf{R}_n^{-1}\mathbf{H}_k'\mathbf{s}_k'\right), \quad (16)$$

where $\mathbf{R}_n$ is the covariance of the noise, which is proportional to the identity matrix. Finally, the power constraint was accounted for by taking the component of the gradient perpendicular to $\mathbf{s}_k'$ as the direction of descent:

$$\nabla_{\mathbf{s}_k'}^{\perp}(\Sigma_k'') = \nabla_{\mathbf{s}_k'}(\Sigma_k'') - \mathbf{s}_k'\frac{(\nabla_{\mathbf{s}_k'}(\Sigma_k''))^T\mathbf{s}_k'}{\mathbf{s}_k'^T\mathbf{s}_k'}. \quad (17)$$

4. MMSE AWD METHOD FOR MOVING TARGETS

To generalise the static target MMSE AWD method to apply to the case where the targets can move, it is necessary to extend the system model to account for this target motion by statistically defining the *actual* variation of the target parameters from one step to the next:

$$\boldsymbol{\theta}_k = \mathbf{f}(\boldsymbol{\theta}_{k-1}, \mathbf{v}_{k-1}), \quad (18)$$

where $\mathbf{f}(.)$ is an arbitrary function and $\mathbf{v}_{k-1}$ is noise, which is independent of $\mathbf{N}_k$ [2]. Importantly, we also define the model for the variation of the target parameters which is available to the MIMO active sensing system:

$$\boldsymbol{\theta}_k = \tilde{\mathbf{f}}(\boldsymbol{\theta}_{k-1}). \quad (19)$$

It can be seen that this has implications for the PF: whereas for the static target case the particles would remain at their initial location throughout, for the moving target case we have that:

$$\boldsymbol{\theta}_k^{(i)} = \tilde{\mathbf{f}}(\boldsymbol{\theta}_{k-1}^{(i)}), \quad (20)$$

[2] in general, the formulation developed in this paper would apply if $\mathbf{f}(.)$ were to change at each step, however for simplicity we fix $\mathbf{f}(.)$

$$\frac{\partial(\mathbf{u}_m^T\mathbf{u}_m)}{\partial s'_{k,n}} = 2\mathbf{u}_m^T\left(\frac{\sum_{i=1}^{N_P} w_k^{(i)}\frac{\partial p(\mathbf{x}_k'^{(m)}|\boldsymbol{\theta}_k^{(i)},\mathbf{s}_k')}{\partial s'_{k,n}}\boldsymbol{\theta}_k^{(i)}}{\sum_{i=1}^{N_P} w_k^{(i)}p(\mathbf{x}_k'^{(m)}|\boldsymbol{\theta}_k^{(i)},\mathbf{s}_k')} - \frac{\left(\sum_{i=1}^{N_P} w_k^{(i)}p(\mathbf{x}_k'^{(m)}|\boldsymbol{\theta}_k^{(i)},\mathbf{s}_k')\boldsymbol{\theta}_k^{(i)}\right)\left(\sum_{i=1}^{N_P} w_k^{(i)}\frac{\partial p(\mathbf{x}_k'^{(m)}|\boldsymbol{\theta}_k^{(i)},\mathbf{s}_k')}{\partial s'_{k,n}}\right)}{\left(\sum_{i=1}^{N_P} w_k^{(i)}p(\mathbf{x}_k'^{(m)}|\boldsymbol{\theta}_k^{(i)},\mathbf{s}_k')\right)^2}\right) \tag{12}$$

if $\tilde{\mathbf{f}}(\cdot)$ requires a random variable, an independent value is drawn for each i.

The ability of the particles to move has profound implications for the operation and effectiveness of the PF. In [13], the particles were placed on a regular grid, because the lack of target parameter variation meant that the particles locations would not vary throughout. However, the dynamic model that we consider herein *does* allow the particle locations to vary, thus we do not need to initialise the PF particles on a grid, and it also means that resampling is beneficial [17, Chapter 3]. The randomised particle initialisation, particle motion and particle resampling can be thought of as the target motion enabling more a more efficient implementation of the PF – as particles are quickly removed from locations of low probability density and re-used at locations of high probability density. This is a generally applicable feature of the PF, however there is also a further computational saving that is specific to our MMSE adaptive waveform design algorithm. To see this, note that the expressions (10) and (12) implicitly use the equality:

$$\hat{\boldsymbol{\theta}}_k \approx \frac{\sum_{i=1}^{N_P} w_k^{(i)}p(\mathbf{x}_k'|\boldsymbol{\theta}_k^{(i)},\mathbf{s}_k')\boldsymbol{\theta}_k^{(i)}}{\sum_{i=1}^{N_P} w_k^{(i)}p(\mathbf{x}_k'|\boldsymbol{\theta}_k^{(i)},\mathbf{s}_k')}. \tag{21}$$

The additional saving is that we can numerically approximate $\hat{\boldsymbol{\theta}}_k$ by averaging over the set of $\boldsymbol{\theta}_k'$ rather than $\boldsymbol{\theta}_k$, that is:

$$\hat{\boldsymbol{\theta}}_k \approx \frac{\sum_{i=1}^{N_S} p(\mathbf{x}_k'|{\boldsymbol{\theta}_k'}^{(i)},\mathbf{s}_k'){\boldsymbol{\theta}_k'}^{(i)}}{\sum_{i=1}^{N_S} p(\mathbf{x}_k'|{\boldsymbol{\theta}_k'}^{(i)},\mathbf{s}_k')}. \tag{22}$$

This can be interpreted as using a subset of the particles at locations of high probability density. Crucially, we now require $\mathcal{O}(N_S^2(Q + LN_TN_R))$ operations for cost function evaluation, rather than $\mathcal{O}(N_SN_P(Q + LN_TN_R))$; and $\mathcal{O}(N_S^2(LN_TQ + L^2N_T^2N_R))$ operations for evaluation of the gradient of the cost function, rather than $\mathcal{O}(N_SN_P(LN_TQ + L^2N_T^2N_R))$. As the number of particles, N_P, no longer appears in the computational complexity expression, a suitably high resolution PF can be used for underlying parameter estimation, without needing to have an adverse effect on the computational complexity of the AWD. Putting together the moving target model and the switch from summing over N_P to summing over N_S, we can replace (7) with:

$$\Sigma_k \approx \Sigma_k''' = \sum_{m=1}^{N_S} \frac{v_m}{\tilde{v}}\tilde{\mathbf{u}}_m^T\tilde{\mathbf{u}}_m, \tag{23}$$

where (replacing (10)):

$$\tilde{\mathbf{u}}_m = \left(\frac{\sum_{i=1}^{N_S} p(\mathbf{x}_k'^{(m)}|\boldsymbol{\theta}_k'^{(i)},\mathbf{s}_k')\boldsymbol{\theta}_k'^{(i)}}{\sum_{i=1}^{N_S} p(\mathbf{x}_k'^{(m)}|\boldsymbol{\theta}_k'^{(i)},\mathbf{s}_k')} - \boldsymbol{\theta}_k'^{(m)}\right). \tag{24}$$

We also express the gradient of the new cost function (replacing (11)):

$$\nabla_{\mathbf{s}_k'}(\Sigma_k''') = \sum_{m=1}^{N_S} \frac{v_m}{\tilde{v}}\nabla_{\mathbf{s}_k'}(\tilde{\mathbf{u}}_m^T\tilde{\mathbf{u}}_m) + \frac{\tilde{v}\nabla_{\mathbf{s}_k'}(v_m) - v_m\nabla_{\mathbf{s}_k'}(\tilde{v})}{\tilde{v}^2}\tilde{\mathbf{u}}_m^T\tilde{\mathbf{u}}_m, \tag{25}$$

where a single element of $\nabla_{\mathbf{s}_k'}(\mathbf{u}_m^T\mathbf{u}_m)$ is expressed in (26) (replacing (12)). Which leads to the final expression for the component of the gradient perpendicular to $\mathbf{s}_k'$ as the directions of descent (replacing (17)):

$$\nabla_{\mathbf{s}_k'}^{\perp}(\Sigma_k''') = \nabla_{\mathbf{s}_k'}(\Sigma_k''') - \mathbf{s}_k'\frac{(\nabla_{\mathbf{s}_k'}(\Sigma_k'''))^T\mathbf{s}_k'}{\mathbf{s}_k'^T\mathbf{s}_k'}. \tag{27}$$

5. NUMERICAL RESULTS

We numerically simulate a MIMO active sensing system with co-located half-wavelength spaced transmit and receive arrays based on the set-up specified in [13, 15]. We set $N_T = N_R = 5$, $L = 1$, $N_S = 250$, $N_P = 1000$ with the threshold for resampling set to 0.9, ASNR $= 0$ dB where ASNR $\triangleq |\alpha|^2\mathrm{P}N_RL/(0.5\sigma_n^2)$ (in which the noise variance, σ_n^2 is the variance of each of the real and imaginary components). We assume that $\boldsymbol{\alpha}$ is known, and all its elements have equal magnitude. We estimate the vector of two unknown target angles $\boldsymbol{\phi}_k$ for $1 \le k \le 30$. We consider two scenarios ($\mathcal{N}(\text{mean}, \text{covariance})$ denotes a multivariate normal):

1. A random walk with no model mismatch: $\boldsymbol{\theta}_k = \mathbf{f}_1(\boldsymbol{\theta}_{k-1}, \mathbf{v}_{k-1}) = \boldsymbol{\theta}_{k-1} + \mathbf{v}_{k-1}$, where $\mathbf{v}_{k-1} \sim \mathcal{N}(\mathbf{0}, \mathbf{I}_2)$; $\tilde{\mathbf{f}}_1 = \mathbf{f}_1$; $\boldsymbol{\theta}_0 = [-70, -10]^T$.
2. The targets move with constant angular velocity, but the MMSE AWD system treats the motion as a random walk $\boldsymbol{\theta}_k = \mathbf{f}_2(\boldsymbol{\theta}_{k-1}) = \boldsymbol{\theta}_{k-1} + [1, -1]^T$; $\tilde{\mathbf{f}}_2 = \tilde{\mathbf{f}}_1$; $\boldsymbol{\theta}_0 = [-80, -21]^T$.

In each case, the root mean squared error (RMSE) was numerically approximated by averaging over 500 trials and the

$$\frac{\partial(\tilde{\mathbf{u}}_m^T\tilde{\mathbf{u}}_m)}{\partial s'_{k,n}} = 2\tilde{\mathbf{u}}_m^T\left(\frac{\sum_{i=1}^{N_S}\frac{\partial p(\mathbf{x}_k'^{(m)}|\boldsymbol{\theta}_k'^{(i)},\mathbf{s}'_k)}{\partial s'_{k,n}}\boldsymbol{\theta}_k'^{(i)}}{\sum_{i=1}^{N_S}p(\mathbf{x}_k'^{(m)}|\boldsymbol{\theta}_k'^{(i)},\mathbf{s}'_k)} - \frac{\left(\sum_{i=1}^{N_S}p(\mathbf{x}_k'^{(m)}|\boldsymbol{\theta}_k'^{(i)},\mathbf{s}'_k)\boldsymbol{\theta}_k'^{(i)}\right)\left(\sum_{i=1}^{N_S}\frac{\partial p(\mathbf{x}_k'^{(m)}|\boldsymbol{\theta}_k'^{(i)},\mathbf{s}'_k)}{\partial s'_{k,n}}\right)}{\left(\sum_{i=1}^{N_S}p(\mathbf{x}_k'^{(m)}|\boldsymbol{\theta}_k'^{(i)},\mathbf{s}'_k)\right)^2}\right) \tag{26}$$

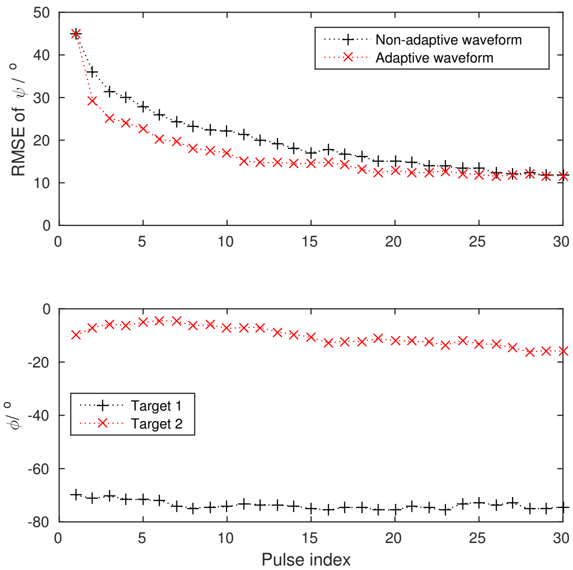

Fig. 1. RMSE and target motion for scenario 1

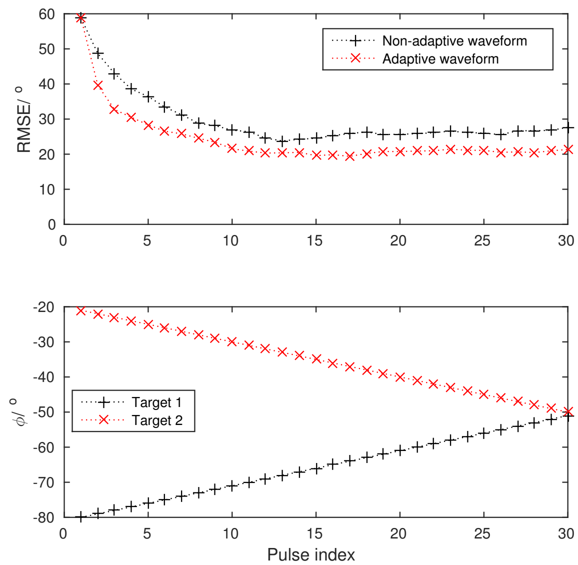

Fig. 2. RMSE and target motion for scenario 2

results are shown in Figs. 1 and 2 for scenarios 1 and 2, respectively. For scenario 1, the reduction in MMSE peaked at 25%, at the 17th pulse; and for scenario 2 the reduction in MMSE peaked at 29%, at the 11th pulse.

The results demonstrate that the MMSE AWD method improves target parameter accuracy both when the system has access to the statistical definition of the target motion (scenario 1) and when there is a model mismatch (scenario 2). To examine the nature of this improvement in a little more detail, it is helpful to think of the estimation as consisting of two parts: an initial target localisation, following by a continuous estimation as the target is tracked. We can see that for both scenarios the MMSE adaptive waveform design method leads to a reduction in RMSE in the target localisation phase, and for scenario 2 there also seems to be a 'steady-state' reduction in target parameter estimation variance. Further results (not included here owing to space constraints) confirm that these two possibilities are typical (i.e., that we always see a reduction in RMSE in target localisation and sometimes in continuous estimation when using MMSE adaptive waveform design), however which occurs is not in general dictated by whether there is a model mismatch (as may be concluded by studying scenarios 1 and 2 alone).

6. CONCLUSIONS

In this paper we have made four main contributions, which together represent an important step towards developing a theoretical method of MMSE AWD which can be implemented in actual MIMO active sensing systems.

- We have extended the analysis in [13] for the case where the active sensing system is tracking moving targets. The formulation we provide includes the possibility of model mismatch.

- We have leveraged the fact that the targets *are* moving to make the algorithm more computationally efficient. Specifically, standard PF techniques of randomised particle initialisation and resampling are used.

- We also introduced the possibility of sampling the particles to estimate the mean of the parameters which yields a further computational saving that is bespoke to our AWD algorithm.

- We have presented numerical results that demonstrate that our AWD algorithm does indeed improve target parameter estimation both with and without a model mismatch.

7. REFERENCES

[1] S. Haykin, "Cognitive radar: a way of the future," *IEEE Signal Processing Magazine*, vol. 23, no. 1, pp. 30–40, Jan 2006.

[2] J. Ender and S. Brüggenwirth, "Cognitive radar - enabling techniques for next generation radar systems," in *2015 16th International Radar Symposium (IRS)*, June 2015, pp. 3–12.

[3] S. P. Sira, Y. Li, A. Papandreou-Suppappola, D. Morrell, D. Cochran, and M. Rangaswamy, "Waveform-agile sensing for tracking," *IEEE Signal Processing Magazine*, vol. 26, no. 1, pp. 53–64, Jan 2009.

[4] W. Huleihel, J. Tabrikian, and R. Shavit, "Optimal adaptive waveform design for cognitive MIMO radar," *IEEE Transactions on Signal Processing*, vol. 61, no. 20, pp. 5075–5089, Oct 2013.

[5] N. Sharaga, J. Tabrikian, and H. Messer, "Optimal cognitive beamforming for target tracking in MIMO radar/sonar," *IEEE Journal of Selected Topics in Signal Processing*, vol. 9, no. 8, pp. 1440–1450, Dec 2015.

[6] M. R. Bell, "Information theory and radar waveform design," *IEEE Transactions on Information Theory*, vol. 39, no. 5, pp. 1578–1597, Sep 1993.

[7] S. Sen and A. Nehorai, "OFDM MIMO radar with mutual-information waveform design for low-grazing angle tracking," *IEEE Transactions on Signal Processing*, vol. 58, no. 6, pp. 3152–3162, June 2010.

[8] A. Turlapaty and Y. Jin, "Bayesian sequential parameter estimation by cognitive radar with multiantenna arrays," *IEEE Transactions on Signal Processing*, vol. 63, no. 4, pp. 974–987, Feb 2015.

[9] R. A. Romero and N. A. Goodman, "Waveform design in signal-dependent interference and application to target recognition with multiple transmissions," *IET Radar, Sonar Navigation*, vol. 3, no. 4, pp. 328–340, August 2009.

[10] G. Rossetti, A. Deligiannis, and S. Lambotharan, "Waveform design and receiver filter optimization for multistatic cognitive radar," in *2016 IEEE Radar Conference (RadarConf)*, May 2016, pp. 1–5.

[11] G. Rossetti and S. Lambotharan, "Waveform optimization techniques for bi-static cognitive radars," in *2016 IEEE 12th International Colloquium on Signal Processing Its Applications (CSPA)*, March 2016, pp. 115–118.

[12] G. Rossetti and S. Lambotharan, "Coordinated waveform design and receiver filter optimization for cognitive radar networks," in *2016 IEEE Sensor Array and Multichannel Signal Processing Workshop (SAM)*, July 2016, pp. 1–5.

[13] S. Herbert, J. Hopgood, and B. Mulgrew, "MMSE adaptive waveform design for active sensing with applications to MIMO radar," *to appear in IEEE Transactions on Signal Processing*, 2017.

[14] A. N. Donev, A. C. Atkinson, and R. D. Tobias, *Optimum Experimental Designs, with SAS*, Oxford Statistical Science Series. Oxford University Press, United Kingdom, 2007.

[15] S. Herbert, J. Hopgood, and B. Mulgrew, "Optimality criteria for adaptive waveform design in MIMO radar systems," in *Sensor Signal Processing for Defence*, Dec 2017.

[16] I. Bekkerman and J. Tabrikian, "Target detection and localization using MIMO radars and sonars," *IEEE Transactions on Signal Processing*, vol. 54, no. 10, pp. 3873–3883, Oct 2006.

[17] B. Ristic, S. Arulampalam, and N. Gordon, *Beyond the Kalman Filter: Particle Filters for Tracking Applications*, Artech House, 2003.